

## Supporting Information

### Ab initio spectroscopy of water under electric field

Giuseppe Cassone<sup>1a</sup>, Jiri Sponer<sup>1b</sup>, Sebastiano Trusso<sup>2c</sup>, Franz Saija<sup>2d</sup>

<sup>1</sup> *Institute of Biophysics of the Czech Academy of Sciences,*

*Královopolská 135, 61265 Brno, Czech Republic*

<sup>2</sup> *CNR-IPCF, Viale Ferdinando Stagno d'Alcontres 37, 98158 Messina, Italy*

(Dated: July 22, 2019)

---

<sup>a</sup> Email: [cassone@ibp.cz](mailto:cassone@ibp.cz)

<sup>b</sup> Email: [sponer@ncbr.muni.cz](mailto:sponer@ncbr.muni.cz)

<sup>c</sup> Email: [trusso@ipcf.cnr.it](mailto:trusso@ipcf.cnr.it)

<sup>d</sup> Email: [saija@ipcf.cnr.it](mailto:saija@ipcf.cnr.it)

## I. RADIAL DISTRIBUTION FUNCTIONS AND DIPOLES ALIGNMENT

From the adherence with the experimental results of the spectra presented in Fig. 1 and Fig. 2 of the main text, along with the correctness of the location and the shapes of the peaks and dips of the zero-field radial distribution functions (RDFs) displayed in Fig. 4 of the main text, we are confident that the employed DFT framework (*i.e.*, BLYP-D3(BJ)) and the statistics gathered with the (long) trajectories and the relatively large size of the simulated box caught remarkably well the relevant features of the liquid water behavior at standard conditions. After all, the size of the simulation box and the temporal length of the current simulations represent a sort of computational upper-bound for such a kind of AIMD numerical experiments under the action of electric fields.

Fig. S1 shows the statistical progressive alignment of the molecular dipole vectors along the field direction.  $\theta$  represents indeed the angle formed by each water dipole moment vector with the field direction (*i.e.*, corresponding to the  $z$ -axis).

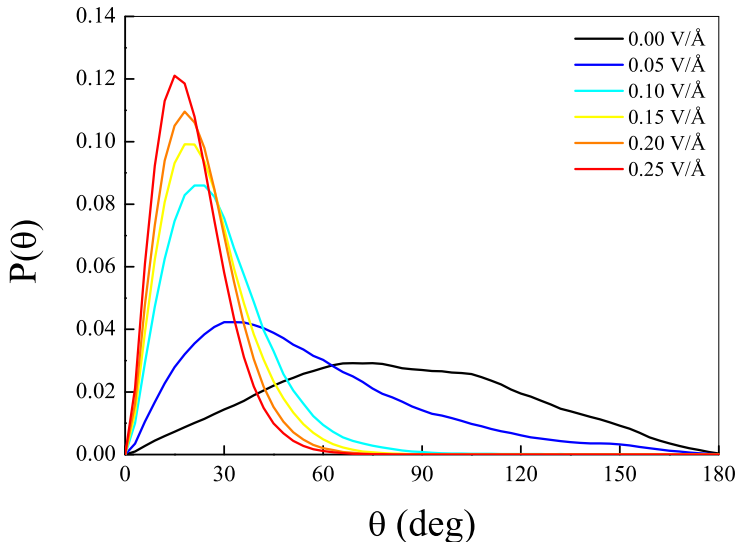


FIG. 1: Distributions of the  $\theta$  angle formed between the vector identifying the water dipole vectors and the field direction from the zero-field regime (black curve) up to 0.25 V/Å (red curve).

$\mathbf{E}$ (V/Å)	$\mathbf{S}_k$
0.00	0.9988946
0.05	0.9988476
0.10	0.9988018
0.15	0.9989043
0.20	0.9988114
0.25	0.9988285

TABLE I: Average value of the translational tetrahedral order parameter  $\mathbf{S}_k$ , as defined in Ref. [1], at zero-field regime (first row) and for different field intensities.

## II. INFRARED AND RAMAN SPECTRA EVALUATION

Both IR and Raman spectra presented in the main text have been determined by means of the software TRAVIS [2, 3] from the centres of the Maximally Localized Wannier Functions (MLWFs) [4, 5] calculated on the fly during the AIMD simulation. In a conventional polarized Raman spectroscopy experiment of liquid water, spectra are acquired with polarization which is either parallel or perpendicular to the incident polarization of the exciting laser. Taking into consideration that theoretical Raman spectra can be obtained from the time autocorrelation functions of the isotropic  $C_{\alpha^2}(t)$  and anisotropic  $C_{\beta^2}(t)$  portions of the water polarizability tensor, the following expressions link the isotropic, anisotropic, perpendicular, parallel and unpolarized Raman scattering spectra [6]:

$$I_{\alpha^2}(\omega) = I_{\parallel}(\omega) - \frac{4}{3}I_{\perp}(\omega) \quad (1)$$

$$I_{\beta^2}(\omega) = \frac{4}{3}I_{\perp}(\omega) \quad (2)$$

$$I_{\perp}(\omega) = \frac{3}{4}I_{\beta^2}(\omega) \quad (3)$$

$$I_{\parallel}(\omega) = I_{\alpha^2}(\omega) + I_{\beta^2}(\omega) \quad (4)$$

$$I_U = I_{\parallel}(\omega) + I_{\perp}(\omega) = I_{\alpha^2}(\omega) + \frac{7}{4}I_{\beta^2}(\omega). \quad (5)$$

The AIMD simulations allow for the evaluation of the  $I_{\parallel}(\omega)$  and  $I_{\perp}(\omega)$  Raman components that can be easily transformed into the isotropic and anisotropic components using Eq.(1) and (2), as shown in Fig. 2 of the main text. Operationally, Raman intensities have been

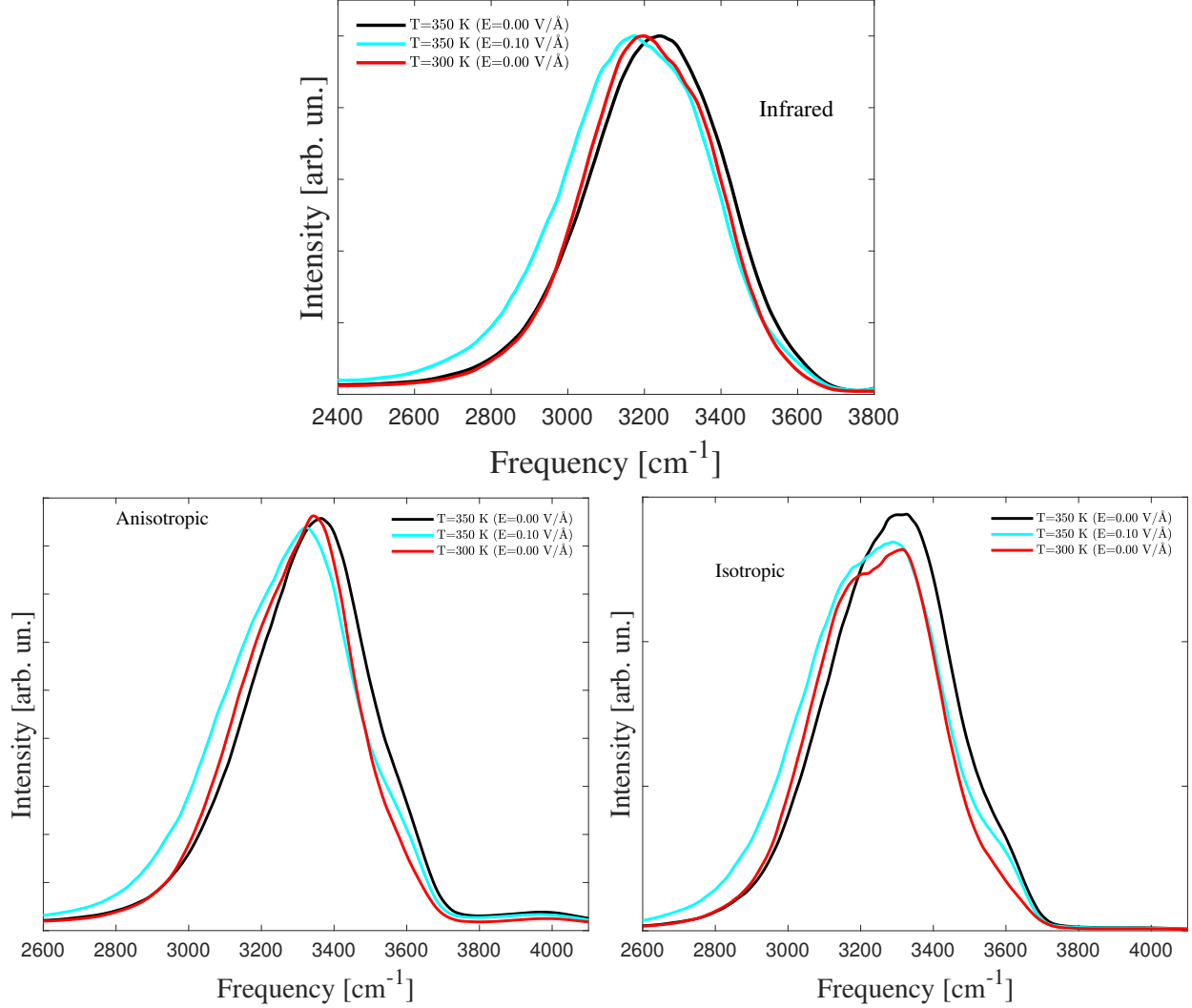


FIG. 2: IR (top panel), anisotropic (left bottom panel), and isotropic (right bottom panel) Raman OH stretching mode bands of bulk liquid water in the zero-field regime at 350 K (black curves), in the zero-field regime at 300 K (red curves), and at 350 K under an electric field strength of  $0.10 \text{ V/\AA}$  (cyan curves).

determined by means of the software TRAVIS [2, 3], exploiting the centres of the MLWFs [4, 5]. In particular, a time-step of 2.5 fs has been chosen for the MLWFs evaluation (*i.e.*, 5 MD time-steps). By employing as a reference the centres of the MLWFs obtained during the AIMD simulations, additional calculations have been executed both for the zero-field regime and for each electric field strength explored. In fact, six calculations per field strength – imposing a relatively small electric field intensity of  $0.0005 \text{ a.u.} \sim 0.026 \text{ V/\AA}$  – (*i.e.*, one

per spatial direction:  $\pm x, \pm y, \pm z$ ) have been carried out in order to obtain the polarizability tensor. From the latter, Raman intensities have been determined and then multiplied by the Bose-Einstein correction  $(1 - \exp(\frac{-\hbar\omega}{k_B T}))$ .

---

- [1] P.-L. Chau and A. J. Hardwick, *Mol. Phys.*, 1998, **93**, 511-518.
- [2] M. Brehm and B. Kirchner, *J. Chem. Inf. Model.*, 2011, **51**, 2007-2023.
- [3] M. Thomas, M. Brehm, R. Fligg, P. Voehringer and B. Kirchner, *Phys. Chem. Chem. Phys.*, 2013, **15**, 6608-6622.
- [4] N. Marzari and D. Vanderbilt, *Phys. Rev. B*, 1997, **56**, 12847-12865.
- [5] N. Marzari, A. A. Mostofi, J. R. Yates, I. Souza and D. Vanderbilt, *Rev. Mod. Phys.*, 2012, **84**, 1419-1475.
- [6] S. R. Pattenaude, L. M. Streacker and D. Ben-Amotz, *J. Raman Spectr.*, 2018, **49**, 1860-1866.